Articles

A Combined QM/MM Approach to Protein−Ligand Interactions: Polarization Effects of the HIV-1 Protease on Selected High Affinity Inhibitors

Christian Hensen,[†] Johannes C. Hermann,[†] Kwangho Nam,[‡] Shuhua Ma,[‡] Jiali Gao,*[,‡] and Hans-Dieter Höltje*[,†]

Institut für Pharmazeutische Chemie, Heinrich-Heine-Universität, Universitätsstrasse 1, 40225 Düsseldorf, Germany, and Department of Chemistry and Supercomputing Institute, Digital Technology Center, University of Minnesota, Minneapolis, Minnesota 55455

Received April 7, 2004

HIV-1 protease inhibitors are one of the two widely used therapeutic agents for the treatment of HIV-infected patients. The investigation of HIV-1 protease−inhibitor interactions can provide further insight for developing new compounds that are still required due to the growing problem of drug resistance. To this end, a combined QM/MM approach was used to determine electrostatic and polarization interactions on three high affinity inhibitors, nelfinavir, mozenavir, and tipranavir. The present computational results show that explicit treatment of the polarization effect is particularly important since it can contribute as much as one-third of the total electrostatic interaction energy. Further, an amino acid decomposition analysis was applied to determine contributions of individual residues to the enzyme−inhibitor interactions. It was found that the 4-hydroxy-dihydropyrone substructure of tipranavir is especially suited for extended charge delocalization by interacting with the catalytic aspartates and isoleucines of the HIV-1 protease. The calculated electron density difference maps reaffirm and provide a means of visualizing these results.

Introduction

The in silico screening of lead compounds in drug discovery relies on computational methods that can rapidly determine properties that include structural features, partition coefficients, and binding interactions.[1−3] Although empirical scoring functions based on two- and three-dimensional quantitative structure−activity relationship (QSAR) and various descriptors are extremely useful, it is desirable, in fact, essential to evaluate binding interactions that include explicit treatment of the ligand, protein, and solvent along with sufficient conformational sampling through Monte Carlo or molecular dynamics (MD) simulations.[4] The latter approach can in principle provide more accurate evaluation of structure−activity relationships and more quantitative estimates of chemical and pharmacological properties. For example, free energy simulation techniques and empirical methods incorporating linear response theory and continuum solvation models can provide quite reliable estimates of relative binding affinities.[3−6] Traditionally, empirical force fields, or molecular mechanics (MM) potential functions, are used to describe protein−ligand and ligand−solvent interactions.[4−6] These potential energy functions, although computationally efficient, must be parametrized and tested for each new ligand compound, which can be time-consuming, and can potentially be the bottleneck for fast screening purposes. On the other hand, quantum mechanical (QM) treatment of the entire protein−ligand−solvent system,[3,7] although does not need parametrization for each new system, is too slow to be practical. Clearly, it is desirable to develop a general approach that is both systematic and computationally efficient for lead-generation and for computation of binding affinities.

In the past 10 years, we have extensively utilized combined quantum mechanical and molecular mechanical (QM/MM) methods to study protein−substrate interactions,[8−10] especially in the context of enzyme catalysis, which concerns the changes in binding free energy of the reactant, transition, and product state. Thus, there is a clear analogy of the computational method used in the study of enzyme reactions and in drug design. In combined QM/MM methods, the ligand/substrate species is treated explicitly by a QM model,[8−10] which, in general, is systematic and can be accurate. The protein and solvent environment is represented by MM force fields, which are computationally efficient. In essence, combined QM/MM methods are ideal for studying protein−ligand interactions in drug discovery because there is no need to parametrize the potential energy function for each new inhibitor, yet the method is computationally efficient and the accuracy of the QM model can be systematically improved. For the latter aspect, it is particularly important because if semiempirical QM model is deemed not applicable for a

* To whom correspondence should be addressed. H.-D.H.: Phone: +49 211 8113661. Fax +49 211 8113847. E-mail: hoeltje@pharm.uni-duesseldorf.de. J.G.: Department of Chemistry, University of Minnesota, 207 Pleasant Street, S.E., Minneapolis, MN 55455. Phone: 612-625-0769. Fax 612-626-7541. E-mail: gao@chem.umn.edu.
[†] Heinrich-Heine-Universität.
[‡] University of Minnesota.

10.1021/jm0497343 CCC: $27.50 © 2004 American Chemical Society
Published on Web 12/02/2004

particular compound, there is always a clear path in quantum mechanics to improve the accuracy through the use of ab initio molecular orbital and density functional theory.

In the present study, we address one specific question, concerning the electronic polarization of the inhibitor by the protein−aqueous environment and its contribution to protein−ligand interactions.[11] Although the importance of polarization effects has long been recognized and there is a continuing effort to develop polarizable force fields for modeling protein−ligand interactions by many research groups, our understanding of the polarization effects and the quantitative contribution to protein−ligand or solute−solvent interactions is still limited.[11] Here, we describe a computational approach to compute polarization energies and to provide qualitative insights into polarization effects on three high-affinity inhibitors to the HIV-1 protease. Although we use a semiempirical QM/MM approach to illustrate the computational procedure, the methodology can be applied to ab initio QM/MM calculations. We further suggest that the results can be useful for making further optimizations of even more potent inhibitors.

The causative agent of the acquired immunodeficiency syndrome (AIDS) disease is the human immunodeficiency virus (HIV). It belongs to a group of retroviruses called lentiviruses and uses cells of the human immune defense as hosts for its replication. HIV requires three viral enzymes encoded by its genome and the protein synthesis machinery of the host cell to reproduce new viruses. The HIV-1 protease (HIV-1 PR) processes the Gag and Pol polypeptides into mature structural proteins and enzymes including the protease itself during the viral lifecycle.[12] The inhibition of the HIV-1 PR activity leads to immature virus particles.[13] Therefore, the interruption of the viral lifecycle through HIV-1 PR inhibitors is a major strategy of the current drug development. However, the therapeutic efficacy is limited because of the growing number of drug resistant HIV-1 PR mutants.[14] Consequently, the HIV protease remains an important target as long as no curative treatment of the AIDS is offered.

The HIV-1 protease is a homodimeric enzyme, and each monomer consists of 99 amino acid residues. The two monomers are related by a 2-fold rotation.[12] The symmetric active site is located at the interface of the two monomers, and amino acids of both chains are involved. Two flaps formed by residues 33−62 and 33′−62′ (monomer B is labeled by an additional apostrophe) control the entry to the binding site, forming a flexible gate for approaching ligands.[15]

The HIV-1 PR belongs to the aspartyl protease family. Accordingly the catalytic center is characterized by two aspartic acids 25/25′ that form a symmetric dyad (Figure 1), which are part of a highly conserved three amino acid sequence, Asp-Thr-Gly in each subunit.[12] The protease preferentially cleaves peptide bonds between Phe and Pro, or Tyr and Pro. The detailed cleavage mechanism is still ambiguous, although many studies support an acid−base mechanism, in which the hybridization of the carbon atom of the peptide bond changes from sp^2 to sp^3 through a nucleophilic attack by a lytic water molecule.[12] Therefore, a monoprotonated catalytic aspartyl dyad is customarily assumed.[16] Current therapeutically used inhibitors block the enzyme by imitating the transition state of the proteolytic process via a hydroxyl group that interacts with the two aspartic acids. On the opposite side of the active site (flap region), two backbone hydrogen atoms from Ile50/50′ are critical for substrate binding, which is mediated by a water molecule (Figure 1).[17,18] Early peptidomimetic protease inhibitors mimic this binding mode.

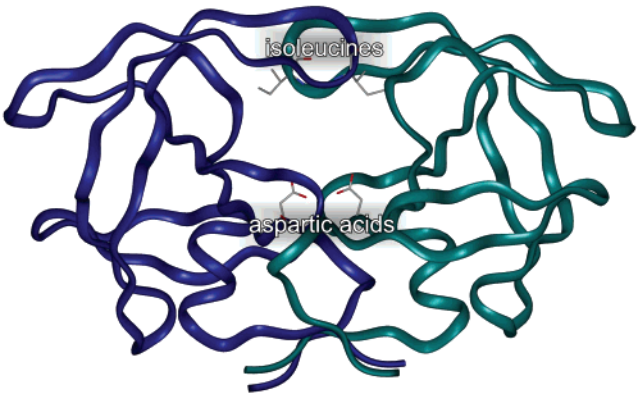

Figure 1. Schematic representation of the HIV-1 protease (PDB entry code 1OHR[17,18]). Ribbons are colored by monomers. Heavy atoms of the catalytic Asp25/25′ and Ile50/50′ are shown in sticks. The active site is located in the center of the indicated amino acids.

Table 1. Structures of the HIV-1 Protease Inhibitors That Are Investigated in This Study[a]

name		K_i [nM]
nelfinavir	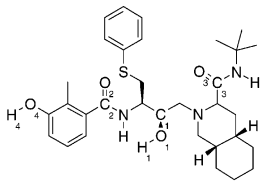	0.28[19]
mozenavir	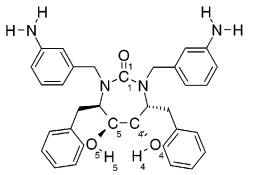	0.41[19]
tipranavir	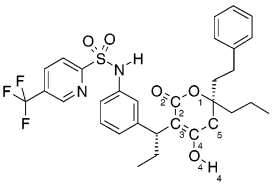	0.008[20]

[a] The atom numbering corresponds to Figure 4.

To elucidate in detail the enzyme inhibition and the interactions between inhibitors and the active site of the enzyme, the effects of the enzyme electric field on the inhibitor were determined. We selected three high affinity inhibitors (Table 1),[19,20] corresponding to different stages of development, to determine the polarization effects of the HIV-1 PR by carrying out an energy decomposition analysis. The therapeutically used inhibitor nelfinavir binds to the enzyme using the water molecule mentioned above, whereas the promising

inhibitors mozenavir (DMP 450) and tipranavir represent modern nonpeptidic structures for the inhibition of the HIV-1 PR that displace this water in the active site. Both inhibitors are in clinical trials. A comparison of the polarization effects among these structures is of great interest for the understanding of the inhibition effects and can be useful for the design of new inhibitors.

Methods

Combined QM/MM methods have been used previously to calculate the electronic polarization effects of organic solutes by solvent and ligand molecules by the protein environment.[8,11] In this approach, the system is partitioned into two regions. The inhibitor is treated quantum mechanically by the semiempirical Austin Model 1 (AM1) method.[21] The surrounding protein amino acids and solvent are approximated by empirical, or molecular mechanical, force fields.[22,23] Since the polarization of the wave function for the ligand is included in the QM/MM calculation,[8] it provides a direct assessment of the energetic contributions to the total inhibitor−protein binding interactions.[11]

The effective Hamiltonian for a QM and MM hybrid system is given as follows:

$$\hat{H} = \hat{H}^0 + \hat{H}_{QM/MM} + \hat{H}_{MM} \quad (1)$$

where $\hat{H}^0$ is the Hamiltonian of the inhibitor, $\hat{H}_{QM/MM}$ represents the interactions between the inhibitor and the enzyme, which includes only electrostatic interactions, and $\hat{H}_{MM}$ denotes the total energy of the MM subsystem of the protein and solvent and the van der Waals interactions between the QM and MM subsystems. The total potential energy for nuclear motions in the combined system is the expectation value of the Hamiltonian:

$$E = \langle \Psi | \hat{H} | \Psi \rangle = E_{QM} + E_{QM/MM} + E_{MM} \quad (2)$$

where Ψ is the electronic wave function of the "QM" inhibitor in the protein. The total interaction energy between a ligand and a protein environment consists of contributions from both the van der Waals and electrostatic terms. For the investigation of the ligand electronic polarization effects, the electrostatic interaction energy is of specific interest, and it is given below:

$$\Delta E_{el} = \langle \Psi | \hat{H}_{QM}{}^0 + \hat{H}_{QM/MM} | \Psi \rangle - \langle \Psi^0 | \hat{H}_{QM}{}^0 | \Psi^0 \rangle = E_{QM} + E_{QM/MM} - E_{QM}{}^0 \quad (3)$$

where Ψ and Ψ^0 refer to the wave functions of the ligand in the protein environment and in the gas phase, respectively. Note that eq 3 defines the electrostatic interaction energy between the ligand molecule with the protein, and it should not be confused with binding energy, which corresponds to the transfer of the ligand from water into the active site.

We use an energy decomposition procedure that was originally developed for the study of small organic compounds in solution[8,24,25] to determine the polarization effects of an inhibitor in the enzyme active site. This approach has recently been used in the study of substrate polarization in the active site of dihydrofolate reductase.[11] The main objective is to decompose the total electrostatic interaction energy into a permanent interaction energy (ΔE_{perm}), corresponding to the interaction of the unpolarized ligand at its gas-phase charge distribution with the enzyme, and a polarization energy (ΔE_{pol}) as a result of the change in the molecular wave function in the active site of the enzyme.[8] Thus, the total electrostatic interaction energy between the inhibitor and the enzyme is written as:

$$\Delta E_{el} = \Delta E_{perm} + \Delta E_{pol} \quad (4)$$

In eq 4, the permanent interaction energy is computed using the wave function of the inhibitor in the gas phase through the QM/MM electrostatic interaction Hamiltonian (this is also called the first-order perturbation energy):

$$\Delta E_{perm} = \langle \Psi^0 | \hat{H}_{QM/MM} | \Psi^0 \rangle \quad (5)$$

The polarization energy can be further decomposed into a polarization stabilization term and an inhibitor electronic distortion term:

$$\Delta E_{pol} = \Delta E_{stab} + \Delta E_{dist} \quad (6)$$

The polarization stabilization energy (ΔE_{stab}) indicates the increase in interaction energy of the inhibitor due to its new charge distribution in the active site. Therefore, this term is always equal to or less than zero, whereas the electronic distortion energy (ΔE_{dist}) refers to the penalty for reorganizing the electron distribution of the inhibitor in the HIV-1 PR active site. The polarization stabilization term is defined by:

$$\Delta E_{stab} = \langle \Psi | \hat{H}_{QM/MM} | \Psi \rangle - \langle \Psi^0 | \hat{H}_{QM/MM} | \Psi^0 \rangle \quad (7)$$

and the electronic distortion is given by:

$$\Delta E_{dist} = \langle \Psi | \hat{H}_{QM}{}^0 | \Psi \rangle - \langle \Psi^0 | \hat{H}_{QM}{}^0 | \Psi^0 \rangle \quad (8)$$

The approach has been previously validated and successfully used in the study of solvation of small molecules,[8,24,25] solvent effects on organic reactions,[9] and substrate−enzyme interactions.[9,11]

Computational Details

The average interaction energies and energy components for nelfinavir, mozenavir, and tipranavir were determined by carrying out MD simulations using a combined QM/MM potential.[8,10c] The semiempirical AM1 model[21] was used for the inhibitor compounds, while the CHARMM22 all-atom force field[22] was adopted for the protein and the three-point charge TIP3P model[23] for water. All simulations were performed using the CHARMM software package.[26] In each case, the crystal structure of the enzyme−inhibitor complex was used as the starting point to construct the computational model.[18,20,27] To mimic the aqueous environment, an equilibrated water sphere of a radius of 25 Å, centered at the geometric center of the inhibitor, was used to solvate the protein−ligand system. Amino acid residues that are more than 25 Å away from the center of the sphere were fixed during the simulations, and atoms in the radial distance range from 20 to 25 Å from the center were harmonically restrained to the initial X-ray crystal positions. The force constants were determined from the *B* factor of the appropriate residues in the crystal structures, multiplied by a scaling factor that increases linearly from zero to one between 20 and 25 Å.[28] Stochastic boundary molecular dynamics method was used for the Langevin dynamics.[28,29] All MD simulations were performed using a time step of 1 fs to

solve the equations of motion. The SHAKE algorithm[30] was used to constrain the bond distances involving hydrogen atoms. Initially, the temperature of the system was gradually raised from 0 to 298 K in 12 ps; subsequently the system was equilibrated by a 250 ps MD simulation at 298 K. The data for the amino acid decomposition analysis was collected in a following 25 ps MD run, whereas data from the next 10 ps simulation time was used for the interaction energy decomposition and the study of the atomic charge polarization. The described computational procedure was applied for all the three investigated ligands. In the presented calculations, a spherical cutoff distance of 12.0 Å was used to calculate the nonbonded interaction energy with a switch function in the region 11.0 to 12.0 Å to feather the interaction energy to zero.

Results and Discussion

A. Interaction Energy Decomposition. The present combined QM/MM molecular dynamics simulations provide an opportunity to analyze the molecular polarization effects of the selected inhibitors as a result of the interactions with the HIV-1 PR. The total electrostatic interaction energies and the described energy components of nelfinavir, mozenavir, and tipranavir are presented in Table 2. The values are averages calculated over 10000 configurations from the 10 ps MD simulations. The polarization energies converge very quickly and they do not fluctuate significantly with longer dynamics simulations. Thus, the relatively short simulation is still reasonable to illustrate the importance of polarization effects. The root-mean-square (RMS) fluctuations of the averages are specified in the table.

Table 2. Electrostatic Interaction Energies and Their Components (kcal/mol) of Nelfinavir, Mozenavir, and Tipranavir with HIV-1 PR from Combined QM/MM Simulations

	nelfinavir	mozenavir	tipranavir
ΔE_{el}	-68.2 ± 0.6	-39.6 ± 0.7	-62.6 ± 1.1
ΔE_{perm}	-46.3 ± 0.5	-24.0 ± 0.7	-39.3 ± 1.1
ΔE_{pol}	-21.9 ± 0.2	-15.5 ± 0.1	-23.3 ± 0.1
ΔE_{stab}	-43.6 ± 0.4	-30.9 ± 0.3	-46.6 ± 0.3
ΔE_{dist}	21.7 ± 0.2	15.4 ± 0.1	23.3 ± 0.1

Table 2 shows that the total electrostatic interaction energies (ΔE_{el}) are of similar magnitude for nelfinavir (68.2 ± 0.6 kcal) and tipranavir (62.6 ± 1.1 kcal), but the electrostatic interaction energy of mozenavir is much smaller (39.6 ± 0.7 kcal). Of course, the computed interaction energies cannot be directly compared with experimental binding constants, which relate to the change in free energy for the transfer of the ligand molecule from water into the enzyme active site. However, since the experimental binding affinities differ only by a factor of 100 among the three inhibitors, the results in Table 2 still demonstrate that electrostatic interactions are more significant in determining binding interactions for nelfinavir and tipranavir than for mozenavir. We attribute this energy difference to the molecular structures in that mozenavir features predominantly hydrophobic interactions involving four aromatic components.

The most striking finding of Table 2 is that electronic polarization of the inhibitor molecules (ΔE_{pol}) by the enzyme environment makes major contributions to the total electrostatic interaction energies, comprising about 32% to 39% of the total electrostatic interaction energy. In comparison with previous studies of molecular polarization of small molecules, which have polarization contributions ranging about 10 to 30% of the total interaction energy,[8,11] the present results have polarization effects in the upper range due to protein polarization. This is understandable in view of the relatively large size of the inhibitor compounds that consist of numerous functional groups that donate and accept hydrogen bonds.

It is interesting to notice that the absolute value of the electronic distortion energy (ΔE_{dist}) is one-half of the absolute value of the polarization stabilization energy (ΔE_{stab}) in each ligand−enzyme complex system. This is consistent with linear response theory, which provides further validation of the computational procedure for interaction energy decomposition.[8,11]

The implication of the present results is that it is essential to consider explicitly electronic polarization effects of the inhibitor to determine ligand−protein interaction energies, and thus, to predict accurately binding free energies. This is because the polarization effects by bulk aqueous solution and the protein active site are expected to be different. Consequently, a frozen permanent charge model would be unrealistic to evaluate interaction energies. We shall present the results of our studies on the differential polarization contributions between aqueous solvation and protein interactions in a future publication.

B. Contributions of Individual Amino Acids. An amino acid decomposition analysis was carried out to investigate major interaction differences among nelfinavir, mozenavir, and tipranavir from individual amino acid residues and to quantify their contributions. Therefore, the average contributions of each residue to the binding energy were determined from a set of 50 coordinates saved at an interval of 0.5 ps from 25 ps MD simulations following the initial equilibration. Contributions were computed by switching off the classical point charges of a particular residue of concern, followed by recalculating the QM/MM energies. The differences of the original and the recalculated energy values are shown in Figure 2. A positive energy change indicates a net reduction of the interaction energy due to the deletion of the charge of an individual amino acid, thereby indicating that the residue makes favorable contributions to inhibitor−protein interactions.

The deprotonated aspartic acid Asp25′ is the most significant residue for enzyme−inhibitor interactions due to a strong hydrogen bond with the hydroxyl group(s) in each inhibitor. In fact, the hydrogen bonding interaction with Asp25′ from a hydroxyl group of the inhibitor is a key feature of HIV-1 protease inhibitors, designed to mimic a similar hydrogen bond from a crystal water. Tipranavir has the largest interaction energy with Asp25′ of the three inhibitors studied. It appears that the 4-hydroxy-dihydropyrone moiety is especially effective in forming hydrogen bonding interactions over the aliphatic secondary hydroxyl groups of nelfinavir and mozenavir. This observation is confirmed by quantitative analysis of the Mulliken population charges in the next section. Interestingly, the protonated Asp25 does not make major contributions to ligand binding; however, it plays a key role in stabilization of Asp25′ and catalysis, and thus it contributes indirectly to inhibitor binding.

The carbonyl group in the central cyclic core of

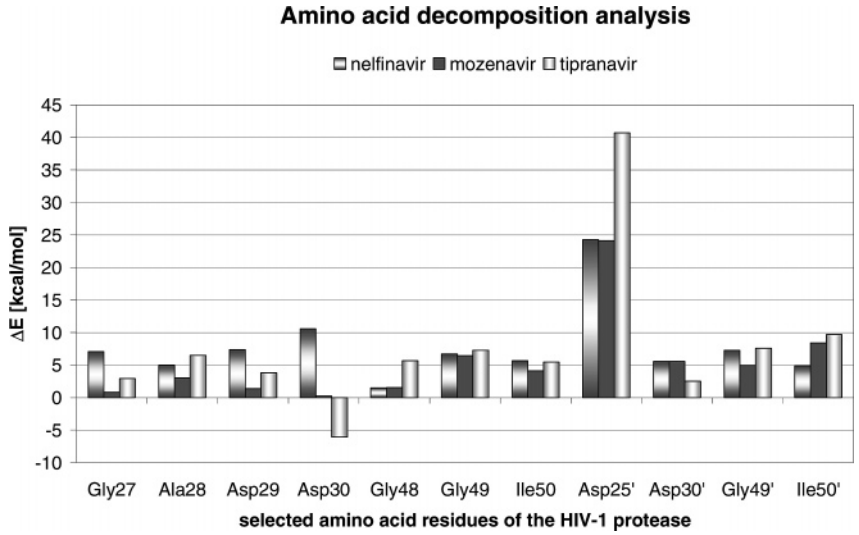

Figure 2. Contributions of individual amino acid residues to inhibitor binding. Positive and negative energy values show the absolute stabilizing or destabilizing effects of selected residues, respectively. Displayed are only residues with an influence of more than 5 kcal/mol to one of the inhibitors.

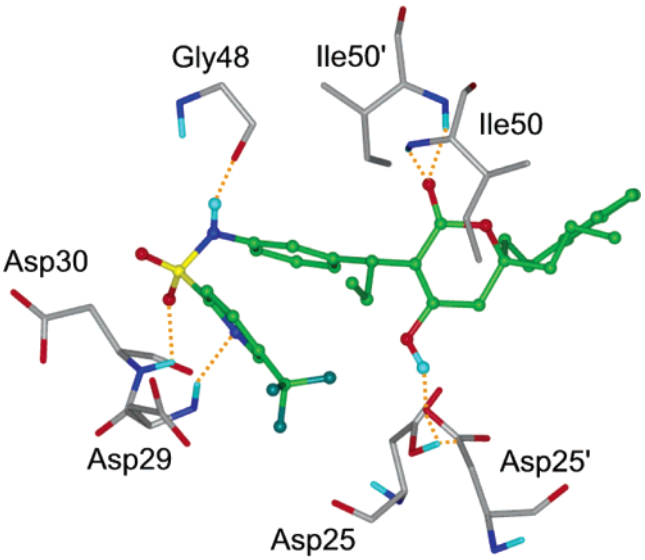

Figure 3. Important hydrogen bond interactions of tipranavir. Tipranavir is represented in ball-and-stick model, the involved amino acids in sticks. Dotted orange lines indicate hydrogen bonds.

mozenavir and tipranavir participates in two hydrogen bonds from the amide groups of Ile50 and Ile50′, and thus, in both systems, these two residues make important contributions to inhibitor binding (Figure 3). In the nelfinavir-HIV-1 PR complex, a water molecule is present to bridge the hydrogen bonds. Residues Ala28, Gly49, and Gly49′ stabilize the three inhibitors in similar ranges.

Asp30 is particularly interesting because of its markedly different effects on the three inhibitor molecules. The interaction energy between Asp30 and mozenavir is essentially negligible, although one of the aromatic amine substructures is located not far from this residue. On the other hand, while Asp30 provides major stabilizing effects on nelfinavir, it destabilizes the interactions with tipranavir. Examining the structures of these complexes from molecular dynamics simulations show that one of the oxygen atoms of the Asp30 carboxyl group forms a hydrogen bond to the nelfinavir H4 atom, whereas in the tipranavir complex, the oxygen atoms of the sulfonamide unit and the Asp30 carboxyl group have repulsive interactions, causing the Asp30 side chain to adopt a different orientation. Figure 3 shows a snapshot of the tipranavir−enzyme complex structure at the active site. The reorientation of the Asp30 carboxyl group occurred during the molecular dynamics equilibration, while one of the oxygen atoms of the sulfonamide group forms a hydrogen bond to the backbone hydrogen atom of Asp30. Thus, we propose that a hydrogen bond donor placed in the oxygen position would enhance the electrostatic interactions of this dihydropyrone derivative.

C. Atomic Charge Polarization. The polarization was also analyzed by computing the partial atomic charges through Mulliken population analysis.[31] Therefore, average atomic charges were computed for the inhibitors in enzymatic environment and in the gas phase during the QM/MM MD simulations. We note that although the calculation of atomic charges is not unique and there are other sophisticated algorithms for deriving atomic charges for molecular systems, the main aim of the present analysis is to illustrate the variation of atomic charges due to molecular polarization. Thus, even though the Mulliken population analysis may not be the most accurate method for computing partial charges, previous studies have shown that the relative change due to charge polarization can still provide meaningful and valuable insight on molecular polarization.[8,11,32] Figure 4 depicts the partial atomic charges on selected polar groups which are important for the ligand binding. Consistent with the discussion on the interactions with Asp25′ in the previous section, the hydroxyl H4 atom of tipranavir exhibits a high degree of polarization as reflected by the large increase in partial positive charge.

We note that the structural features of the cyclic dihydropyrone ring are perfectly suited for charge polarization, resembling a push−pull mechanism, through interactions with Asp25/25′, which push electron density away, and with Ile50/50′, which attract electron density toward the carbonyl group. The π-con-

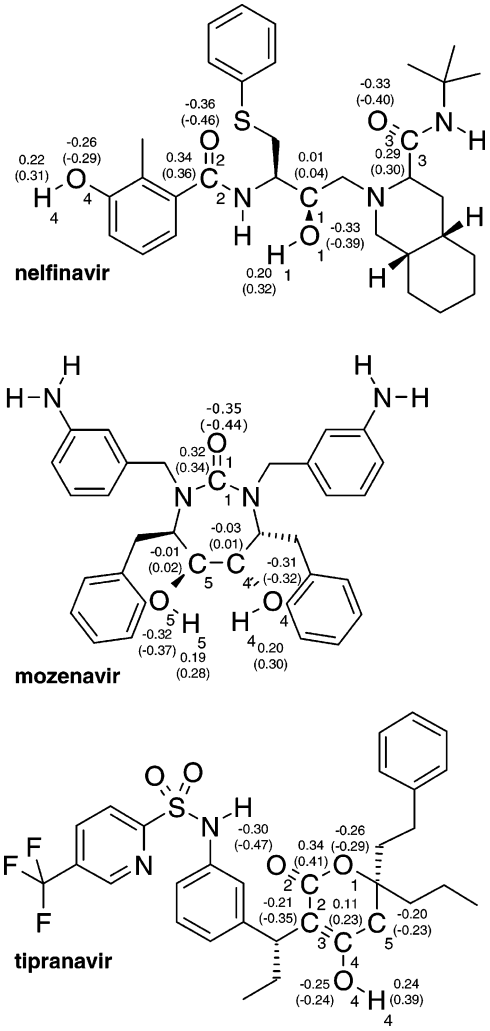

Figure 4. Average partial atomic charges in the gas phase and in the enzyme (in parentheses). Values are given in atomic units (a.u.) for selected atoms. The RMS fluctuations of the presented charges are in the range 0.01−0.03 a.u.

jugated system allows efficient charge delocalization over a significant structural range as shown in Figure 4. This structural element seems much more favorable than the secondary aliphatic hydroxyl groups of nelfinavir and mozenavir. From these results, it can be deduced that the dihydropyrone substructure is the main reason for the high binding affinity of tipranavir, partially due to the mesomeric activation of the hydroxyl group.

D. Charge Density. The charge polarization effects of the HIV-1 PR on its inhibitors are illustrated by visualization of electron density changes, which are determined using a method previously described and successfully applied for several systems.[8,11,32] We determine the wave functions for the ligand molecule in the complex configuration both in the gas phase and in the enzyme active site, from which the total electron densities in the two environments are calculated. The difference between these two electron densities provides a direct indication of the charge migration due to polarization. Therefore, changes in the electron density of each inhibitor resulting from electrostatic interactions with the enzyme are determined. The electron density difference (EDD) plots for representative structures of

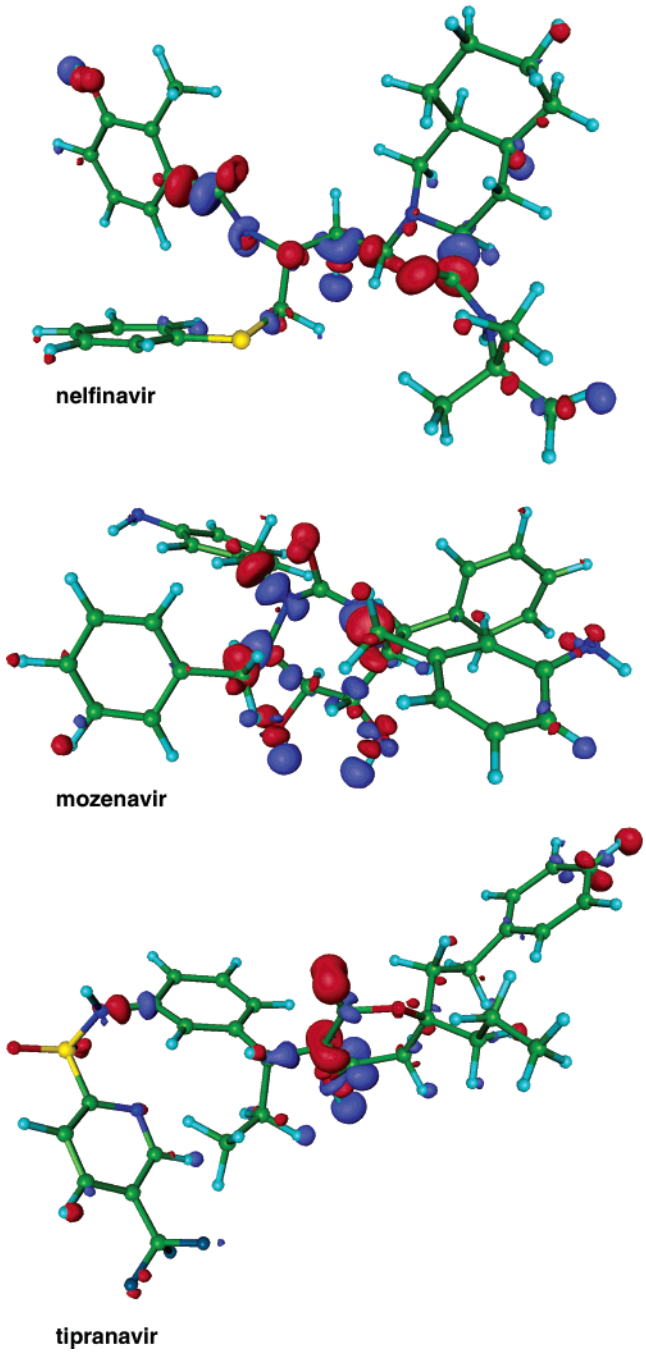

Figure 5. Electron density difference plots for the inhibitors nelfinavir, mozenavir, and tipranavir. Blue contoured regions indicate a depletion of electron density; red contoured regions represent areas where the electron density increases. The contours are generated at the same contour level. The relative orientation of the atoms is comparable to Figure 4.

the three inhibitors are shown in Figure 5. Red and blue contours illustrate the gains and losses of electron density due to the change of environment from the gas phase into the active site of HIV-1 protease. These plots mirror the quantitative findings from atomic charge polarization analysis. Clearly seen are major polarization effects of the inhibitors arising from electrostatic interactions at polar groups. In particular blue contours near the hydrogen atoms of the hydroxyl groups show depletion of electron density due to donating a hydrogen bond to Asp25′, whereas the electron density on the oxygen atom concomitantly increases. The large gains

of the electron density on nelfinavir's O2 and O3 atoms, mozenavir's O1 atom, and tipranavir's O2 atom confirm the role of significant interactions with Ile50 and Ile50′. Figure 5 also illustrates the conjugative charge polarization through the dihydropyrone ring of tipranavir.

The plot of nelfinavir shows as well a high polarized area on the H4 and O4 atoms that form a hydrogen bond to the carboxyl group of Asp30. The quantitative gain of interaction energy due to this hydrogen bond is given in Figure 2.

Conclusions

Combined QM/MM molecular dynamics simulations have been carried out with three high affinity HIV-1 PR inhibitors to provide a deeper understanding of the origin of enzyme−ligand interactions. This will in turn help to develop more accurate scoring functions for prediction of binding free energies in drug discovery. Quantitative polarization energies are determined as averages from molecular dynamics simulations, in which the inhibitor is treated explicitly by a quantum mechanical model. The results lead to the conclusion that polarization is a crucial component of the electrostatic enzyme−inhibitor interactions that comprise about one-third to the total electrostatic interaction energy. The data show that frozen permanent charge models would be unrealistic to determine interaction energies and the consideration of explicit polarization terms is required for the reliable prediction of binding free energies.

Technically, an important and useful feature of the combined QM/MM method is that it can, in principle, be applied to any new ligand compounds without the need to develop specific empirical parameters, and consequently, it can provide a systematic evaluation of binding interactions for a series of compounds. This is particularly advantageous over methods that make use of empirical partial charges. The use of a semiempirical QM model allows large ligand molecules such as those investigated in the present work to be studied. We believe that even though the accuracy of semiempirical methods for conformational energy calculations can be further improved, their use for estimating polarization effects and energies is accurate as demonstrated by numerous studies in comparison with ab initio QM/MM simulations.[8,11,24,25,32] The present investigation illustrates the applicability of combined QM/MM methods for future calculations of molecular polarization and its potential for reliably predicting absolute and relative binding free energies.

In addition, the amino acid decomposition analysis provides further insight into the effects of individual amino acid residues on ligand binding, and the information can be useful for designing novel inhibitors that take advantage of conjugative charge polarizations. The polarization effects can be quantified energetically, by comparison with charge population analysis and by qualitative visualization of charge migrations. For the HIV-1 PR-inhibitor complexes investigated in the present study, the estimated polarization and energetic results confirm that the 4-hydroxy-dihydropyrone substructure of tipranavir is a most effective structural arrangement that enhances polarization effects. This is achieved through a push−pull mechanism involving donating a hydrogen bond to the catalytic Asp25/25′ on one side of the ring and accepting two hydrogen bonds from the amide groups of Ile50/50′. This key structural element is attributed to a main reason responsible for tipranavir's high binding affinity to the HIV-1 PR. As the most important effect of these improved binding interactions, the risk of loss of efficacy due to mutations is significantly reduced. Of course, a mutation of the catalytic aspartates 25/25′ would result in a noneffective enzyme, thus not of a concern in drug design. In addition, we propose that a hydrogen bond donor instead of the sulfonamide substructure of tipranavir would enhance electrostatic interactions with Asp30, thereby further increasing the binding affinity of tipranavir.

Acknowledgment. We thank the National Institutes of Health (J.G.) and Riemser Arzneimittel AG (H.D.H.) for support of this research. C.H. is grateful for the generous hospitality and the extensive scientific support by Professor J. Gao during his stay at the Department of Chemistry, University of Minnesota, Minneapolis.

References

(1) Jorgensen, W. L. The many roles of computation in drug discovery. *Science* **2004**, *303*, 1813−1818.
(2) Meng, E. C.; Shoichet, B. K.; Kuntz, I. D. Automated docking with grid-based energy evaluation. *J. Comput. Chem*. **1992**, *13*, 505−524.
(3) Raha, K.; Merz, K. M., Jr. A quantum mechanics-based scoring function: Study of zinc ion-mediated ligand binding. *J. Am. Chem. Soc.* **2004**, *126*, 1020−1021.
(4) Kollman, P. A. Free energy calculations: Applications to chemical biochemical phenomena. *Chem. Rev*. **1993**, *93*, 2395−2417.
(5) Åqvist, J.; Medina, C.; Samuelsson, J. E. A new method for predicting binding affinity in computer-aided drug design. *Protein Eng*. **1994**, *7*, 385−391.
(6) Rizzo, R. C.; Udier-Blagovic, M.; Wang, D.-P.; Watkins, E. K.; Kroeger-Smith, M. B.; Smith, R. H., Jr.; Tirado-Rives, J.; Jorgensen, W. L. Prediction of activity for nonnucleoside inhibitors with HIV-1 reverse transcriptase based on Monte Carlo simulations. *J. Med. Chem*. **2002**, *45*, 2970−2987.
(7) Khandogin, J.; York, D. M. Quantum Mechanical Characterization of Nucleic Acids in Solution: A Linear-Scaling Study of Charge Fluctuations in DNA and RNA. *J. Phys. Chem. B* **2002**, *106*, 7693−7703.
(8) Gao, J.; Xia, X. A Priori Evaluation of Aqueous Polarization Effects Through Monte Carlo QM-MM Simulations. *Science* **1992**, *258*, 631−635.
(9) (a) Gao, J. Methods and applications of combined quantum mechanical and molecular mechanical potentials. *Rev. Comput. Chem.* **1995**, *7*, 119−185. (b) Gao, J. Hybrid Quantum and Molecular Mechanical Simulations: An Alternative Avenue to Solvent Effects in Organic Chemistry. *Acc. Chem. Res*. **1996**, *29*, 298−305. (c) Gao, J.; Truhlar. D. G. Quantum Mechanical Methods for Enzyme Kinetics. *Annu. Rev. Phys. Chem*. **2002**, *53*, 467−505.
(10) (a) Warshel, A.; Levitt, M. Theoretical studies of enzymic reactions: dielectric, electrostatic and steric stabilization of the carbonium ion in the reaction of lysozyme. *J. Mol. Biol*. **1976**, *103*, 227−249. (b) Singh, U. C.; Kollman, P. A. A combined ab initio quantum mechanical and molecular mechanical method for carrying out simulations on complex molecular systems: applications to $CH_3Cl + Cl^-$ exchange reaction and gas-phase protonation of polyethers. *J. Comput. Chem.* **1986**, *7*, 718−730. (c) Field, M. J.; Bash, P. A.; Karplus, M. A Combined Quantum-Mechanical and Molecular Mechanical Potential for Molecular-Dynamics Simulations. *J. Comput. Chem.* **1990**, *11*, 700−733.
(11) Garcia-Viloca, M.; Truhlar, D. G.; Gao, J. Importance of substrate and cofactor polarization in the active site of dihydrofolate reductase. *J. Mol. Biol.* **2003**, *327*, 549−560.
(12) Huff, J. R. HIV protease: a novel chemotherapeutic target for AIDS. *J. Med. Chem.* **1991**, *34*, 2305−2314.
(13) Kohl, N. E.; Emini, E. A.; Schleif, W. A.; Davis, L. J.; Heimbach, J. C.; Dixon, R. A.; Scolnick, E. M.; Sigal, I. S. Active human immunodeficiency virus protease is required for viral infectivity. *Proc. Natl. Acad. Sci. U.S.A.* **1988**, *85*, 4686−4690.
(14) Deeks, S. G. Treatment of antiretroviral-drug-resistant HIV-1 infection. *Lancet* **2003**, *362*, 2002−2011.

(15) Scott, W. R. P.; Schiffer, C. A. Curling of Flap Tips in HIV-1 Protease as a Mechanism for Substrate Entry and Tolerance of Drug Resistance. *Structure* **2000**, *8*, 1259−1265.
(16) Hyland, L. J.; Tomaszek, T. A., Jr.; Meek, T. D. Human immunodeficiency virus-1 protease. 2. Use of pH rate studies and solvent kinetic isotope effects to elucidate details of chemical mechanism. *Biochemistry* **1991**, *30*, 8454−8463.
(17) Berman, H. M.; Westbrook, J.; Feng, Z.; Gilliland, G.; Bhat, T. N.; Weissig, H.; Shindyalov, I. N.; Bourne, P. E. The Protein Data Bank. *Nucleic Acids Res.* **2000**, *28*, 235−242.
(18) Kaldor, S. W.; Kalish, V. J.; Davies, J. F., II.; Shetty, B. V.; Fritz, J. E.; Appelt, K.; Burgess, J. A.; Campanale, K. M.; Chirgadze, N. Y.; Clawson, D. K.; Dressmann, B. A.; Hatch, S. D.; Khalil, D. A.; Kosa, M. B.; Lubbehusen, P. P.; Muesing, M. A.; Patick, A. K.; Reich, S. H.; Su, K. S.; Tatlock, J. H. Viracept (Nelfinavir Mesylate, AG1343): A Potent, Orally Bioavailable Inhibitor of HIV-1 Protease. *J. Med. Chem.* **1997**, *40*, 3979−3985.
(19) Klabe, R. M.; Bacheler, L. T.; Ala, P. J.; Erickson-Viitanen, S. E.; Meek, J. L. Resistance to HIV protease inhibitors: a comparison of enzyme inhibition and antiviral potency. *Biochemistry* **1998**, *37*, 8735−8742.
(20) Thaisrivongs, S.; Skulnick, H. I.; Turner, S. R.; Strohbach, J. W.; Tommasi, R. A.; Johnson, P. D.; Aristoff, P. A.; Judge, T. M.; Gammill, R. B.; Morris, J. K.; Romines, K. R.; Chrusciel, R. A.; Hinshaw, R. R.; Chong, K.-T.; Tarpley, W. G.; Poppe, S. M.; Slade, D. E.; Lynn, J. C.; Horng, M.-M.; Tomich, P. K.; Seest, E. P.; Dolak, L. A.; Howe, W. J.; Howard, G. M.; Schwende, F. J.; Toth, L. N.; Padbury, G. E.; Wilson, G. J.; Shiou, L.; Zipp, G. L.; Wilkinson, K. F.; Rush, B. D.; Ruwart, M. J.; Koeplinger, K. A.; Zhao, Z.; Cole, S.; Zaya, R. M.; Kakuk, T. J.; Janakiraman, M. N.; Watenpaugh, K. D. Structure-Based Design of HIV Protease Inhibitors: Sulfonamide-Containing 5,6-Dihydro-4-hydroxy-2-pyrones as Non-Peptidic Inhibitors. *J. Med. Chem.* **1996**, *39*, 4349−4353.
(21) Dewar, M. J. S.; Zoebisch, E. G.; Healy, E. F.; Stewart, J. J. P. Development and use of quantum mechanical molecular models. 76. AM1: a new general purpose quantum mechanical molecular model. *J. Am. Chem. Soc*. **1985**, *107*, 3902−3909.
(22) MacKerell, A. D., Jr.; Bashford, D.; Bellott, R. L.; Dunbrack, R. L., Jr.; Evanseck, J. D.; Field, M. J.; Fischer, S.; Gao, J.; Guo, H.; Ha, S.; Joseph-McCarthy, D.; Kuchnir, L.; Kuczera, K.; Lau, F. T. K.; Mattos, C.; Michnick, S.; Ngo, T.; Nguyen, D. T.; Prodhom, B.; Reiher, W. E., III.; Roux, B.; Schlenkrich, M.; Smith, J. C.; Stote, R.; Straub, J.; Watanabe, M.; Wiorkiewicz-Kuczera, J.; Yin, D.; Karplus, M. All-Atom Empirical Potential for Molecular Modeling and Dynamics Studies of Proteins. *J. Phys. Chem. B* **1998**, *102*, 3586−3616.
(23) Jorgensen, W. L.; Chandrasekhar, J.; Madura, J. D.; Impey, R. W.; Klein, M. L. Comparison of simple potential functions for simulating liquid water. *J. Chem. Phys.* **1983**, *79*, 926−935.
(24) Gao, J. The hydration and solvent polarization effects of nucleotide bases. *Biophys. Chem.* **1994**, *51*, 253−261.
(25) Cubero, E.; Luque, F. J.; Orozco, M.; Gao, J. Perturbation Approach to Combined QM/MM Simulaiton of Solute−Solvent Interactions in Solution. *J. Phys. Chem. B* **2003**, *107*, 1664−1671.
(26) Brooks, B. R.; Bruccoleri, R. E.; Olafson, B. D.; States, D. J.; Swaminathan, S.; Karplus, M. CHARMM: a program for macromolecular energy, minimization, and dynamics calculations. *J. Comput. Chem.* **1983**, *4*, 187−217.
(27) Hodge, C. N.; Aldrich, P. E.; Bacheler, L. T.; Chang, C. H.; Eyermann, C. J.; Garber, S.; Grubb, M.; Jackson, D. A.; Jadhav, P. K.; Korant, B.; Lam, P. Y. S.; Maurin, M. B.; Meek, J. L.; Otto, M. J.; Rayner, M. M.; Reid, C.; Sharpe, T. R.; Shum, L.; Winslow, D. L.; Erickson-Viitanen, S. Improved cyclic urea inhibitors of the HIV-1 protease: synthesis, potency, resistance profile, human pharmacokinetics and X-ray crystal structure of DMP 450. *Chem. Biol.* **1996**, *3*, 301−314.
(28) Brooks, C. L., III.; Brünger, A.; Karplus, M. Active site dynamics in protein molecules: a stochastic boundary molecular-dynamics approach. *Biopolymers* **1985**, *24*, 843−865.
(29) Brooks, C. L., III.; Karplus, M. Solvent effects on protein motion and protein effects on solvent motion. Dynamics of the active site region of lysozyme. *J. Mol. Biol*. **1989**, *208*, 159−181.
(30) Ryckaert, J. P.; Ciccotti, G.; Berendsen, H. J. C. Numerical Integration of Cartesian Equations of Motion of a System with Constraints: Molecular Dynamics of *n*-Alkanes. *J. Comput. Phys.* **1977**, *23*, 327−341.
(31) Mulliken, R. S. Electronic population analysis on LCAO-MO molecular wave functions .1. *J. Chem. Phys.* **1955**, *23*, 1833−1840.
(32) Mo, Y.; Subramanian, G.; Gao, J.; Ferguson, D. M. Cation-π Interactions: An Energy Decomposition Analysis and Its Implication in δ-Opioid Receptor−Ligand Binding. *J. Am. Chem. Soc.* **2002**, *124*, 4832−4837.

JM0497343